

Preparation, Crystal Structures, and Spectroscopic and Redox Properties of Nickel(II) Complexes Containing Phosphane–(Amine or Quinoline)-Type Hybrid Ligands and a Nickel(I) Complex Bearing 8-(Diphenylphosphanyl)quinoline

Akira Hashimoto,^[a] Hiroshi Yamaguchi,^[a] Takayoshi Suzuki,^{*[b]} Kazuo Kashiwabara,^[a] Masaaki Kojima,^[b] and Hideo D. Takagi^{*[a]}

Keywords: N,P ligands / Nickel / Phosphane ligands / Ligand effects

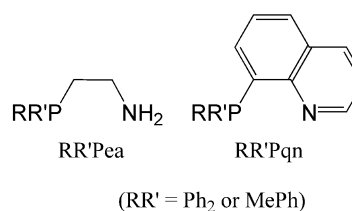
Nickel(II) complexes containing P–N-type bidentate hybrid ligands of 2-aminoethylphosphanes (RR'Pea; RR' = Ph₂ or MePh) or 8-quinolyphosphanes (RR'Pqn), namely [Ni(P–N)₂](BF₄)₂ [P–N = Ph₂Pea (**1**), MePhPea (**2**), Ph₂Pqn (**3**), or MePhPqn (**4**)] have been prepared, and their structural, spectroscopic, and electrochemical properties determined. The crystal structure analysis indicates that the 2-aminoethylphosphane complexes (**1** and **2**) have a square-planar coordination geometry around the Ni^{II} center with a *cis*(*P,P*) configuration, whereas the 8-quinolyphosphane complexes (**3** and **4**) exhibit a severe tetrahedral distortion because of the steric repulsion between the *ortho*-H atoms in the mutually *cis*-positioned quinolyl rings. Complexes **1** and **2** maintain their

diamagnetic square-planar four-coordinate structure on acetonitrile solution, whereas complexes **3** and **4** show paramagnetic behavior. Spectroscopic and electrochemical measurements suggest that the ligand-field strengths of these four P–N-type ligands increase in the order Ph₂Pqn (**3**) < MePhPqn (**4**) < Ph₂Pea (**1**) < MePhPea (**2**). The Ph₂Pqn complex **3** is readily reduced by Zn powder to afford the corresponding nickel(I) complex [Ni(Ph₂Pqn)₂](BF₄)₂ (**5**). The crystal structure of complex **5** reveals that the Ni^I ion adopts a distorted tetrahedral coordination geometry with slightly longer (≈ 0.05 Å) Ni–P and Ni–N bond lengths than those in the corresponding Ni^{II} complex **3**.

Introduction

Transition-metal complexes containing hybrid-type hemilabile phosphane ligands^[1] have recently attracted a great deal of interest in applications as wide ranging as effective chemosensors for small molecules,^[2] homogeneous catalysts for the activation of inert small molecules,^[3] anticancer agents,^[4] and so on.^[5] In order to develop novel functionalities and catalytic and biological activities for these complexes, it is essential to design the electronic differentiations^[1b,1c] of the donor groups as well as the steric requirements of the hybrid-type ligands. In this respect, we are currently focusing our attention on P–N-type hybrid ligands bearing an amine or pyridine/quinoline donor group and the investigation of their coordination behavior.^[6–11] Herein we consider nickel(II) complexes having 2-amino-

ethylphosphanes (RR'Pea) or 8-quinolyphosphanes (RR'Pqn) (Scheme 1), which are P–N-type bidentate ligands that form a five-membered chelate ring.



Scheme 1. P–N-type ligands used in this study.

Several transition-metal complexes with (2-aminoethyl)diphenylphosphane (Ph₂PCH₂CH₂NH₂; Ph₂Pea) have been prepared^[12–14] since the first reports by Issleib and co-workers.^[15] In contrast, complexes of the analogous P–N-type ligand having an asymmetric phosphorus donor atom, namely (2-aminoethyl)methylphenylphosphane (MePhPCH₂CH₂NH₂; MePhPea), are limited to those of cobalt(III),^[12c] palladium(II), and platinum(II).^[16] Moreover, studies on the molecular structures and properties of metal complexes with 8-quinolyphosphanes are also scarce.^[7–9,17,18] As an example, one of the present authors (T.S.) has reported a novel crystal modification of *cis*(*P,P*)-

[a] Graduate School of Science and Research Center for Materials Science, Nagoya University, Furocho, Chikusa, Nagoya 464-8602, Japan
Fax: +81-52-789-5473
E-mail: h.d.takagi@nagoya-u.jp

[b] Department of Chemistry, Faculty of Science, Okayama University, Tsushima-naka 3-1-1, Okayama 700-8530, Japan
Fax: +81-86-251-7900
E-mail: suzuki@cc.okayama-u.ac.jp

Supporting information for this article is available on the WWW under <http://dx.doi.org/10.1002/ejic.200900767>.

[Pd(Ph₂Pqn)₂]₂Br₂ (yellow blocks vs. orange prisms) and its chloride and/or tetrafluoroborate salts, which could be related to a tetrahedral distortion of the coordination plane of Pd^{II} because of the intramolecular steric interaction between two mutually *cis*-positioned quinolyl groups.^[8] For the corresponding Ni^{II} complexes, including those of the related P–N-type hybrid ligands,^[19] there are very limited reports on structural determinations and spectroscopic characterization of the complexes. We have previously described the syntheses and structures of [Ni(Me₂Pea)₂]Cl₂, [Ni(Me₂Pea)₂][NiCl₄] (where Me₂Pea was previously abbreviated as edmp),^[6] and [Ni(Me₂Pqn)₂](BF₄)₂.^[7] Herein we report the syntheses, structural analyses, and spectroscopic and electrochemical properties of the Ni^{II} complexes [Ni(P–N)₂](BF₄)₂ containing Ph₂Pea (**1**), MePhPea (**2**), Ph₂Pqn (**3**), or MePhPqn (**4**) as the P–N ligand (Scheme 1). The corresponding Ni^I complex, [Ni(Ph₂Pqn)₂]BF₄ (**5**), prepared by reduction of complex **3** with Zn powder, is also described.

Results and Discussion

Preparation and Crystal Structures of Nickel(II) Complexes

The nickel(II) complexes [Ni(P–N)₂](BF₄)₂ (**1–4**) were prepared from Ni(BF₄)₂·6H₂O and a small excess of P–N ligand in methanol or ethanol following a similar method to that used to obtain [Ni(Me₂Pea or Me₂Pqn)₂](BF₄)₂.^[6,7] [Ni(Ph₂Pea)₂](BF₄)₂ (**1**) was obtained analytically pure, and magnetic susceptibility measurements at room temperature indicated that this complex is diamagnetic. The ¹H NMR spectrum of **1** (in CD₃CN) shows all resonances in the normal diamagnetic region, although the resonances of the 2-aminoethyl moieties (PCH₂CH₂NH₂) are remarkably broad, presumably because of the puckering motion of the chelate ring. The molecular structure of complex **1** was determined by single-crystal X-ray analysis; a perspective view of the divalent Ni^{II} complex cation in **1** is given in Figure 1. The coordination geometry around the Ni^{II} center was confirmed as four-coordinate square planar with a *cis*(*P,P*) configuration. It is known that the *cis*(*P,P*) isomer is electronically favored when two phosphanyl-donor groups having a strong *trans* influence coordinate to a square-planar metal center, although it is sterically disfavored when the phosphanyl-donor groups bear bulky substituents on the P atom.^[6] The present result indicates that the electronic effect, in other words the *trans* influence, is more important for the Ni^{II} complexes, and that the steric interaction between the phenyl substituents may be reduced efficiently by a pair of conformations of two 2-aminoethylphosphane chelate rings (see below).

Complex **2**, which contains MePhPea, was expected to have a similar coordination geometry because the related complex [Ni(Me₂Pea)₂](BF₄)₂ was also obtained as a *cis*(*P,P*) isomer.^[6] However, complex **2** can form two possible diastereoisomers (*rac* and *meso*) due to the pair of asymmetric P atoms. The crude product isolated from the reaction mixture was found to have the composition Ni-

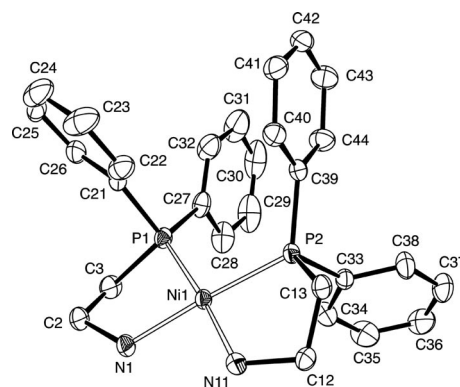


Figure 1. An ORTEP view (50% probability level, hydrogen atoms omitted) of the cationic moiety in [Ni(Ph₂Pea)₂](BF₄)₂ (**1**).

(MePhPea)₂(BF₄)₂, although its ¹H NMR spectrum (in CD₃CN) was indicative of a mixture of two isomers (Figure S1). These isomers were separated on the basis of their different solubilities in dichloromethane, and the crystal structure of the less soluble product was determined by X-ray analysis. As seen from Figure 2, the analyzed complex is assigned as the *racemic* (*RR/SS*) diastereoisomer (abbreviated as *rac-2*).

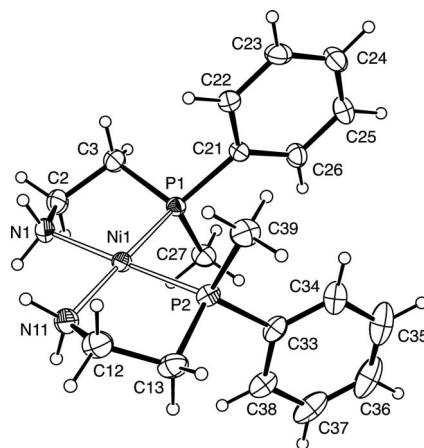


Figure 2. An ORTEP view (50% probability level) of the cationic moiety in *rac*-[Ni(MePhPea)₂](BF₄)₂ (*rac-2*). Note that the illustrated complex is assigned as an *SS* stereoisomer; however, this compound crystallized in the centrosymmetric space group *P* $\bar{1}$.

Complexes **1** and **2** show an ideal planar coordination geometry around the Ni atom. The largest deviation of the constituent atoms from the ideal plane defined by {Ni1,P1,P2,N1,N11} was only 0.023(2) Å (**1** for N11) or 0.131(3) Å (**2** for N11). For both complexes, a pair of conformations of the five-membered 2-aminoethylphosphane chelate rings was determined as $\delta\delta/\lambda\lambda$ (*racemic*). This conformation, with a pseudo-*C*₂ molecular symmetry, would be the most favorable for reducing the intramolecular steric interactions in the *cis*(*P,P*) isomer, although a different pair of ring conformations was observed in the analogous Me₂-Pea complexes.^[6] A weak interaction exists between the metal(II) ion and the chloride in the crystal structures of

$[\text{Ni}(\text{Me}_2\text{Pea})_2]\text{Cl}_2$ and its Pd^{II} and Pt^{II} analogues, and the pair of ring conformations of the Me_2Pea chelates was found to be $\delta\lambda$ (*meso*), with a pseudo- C_s molecular symmetry. In contrast, the crystal structure of $[\text{Ni}(\text{Me}_2\text{Pea})_2][\text{NiCl}_4]$ did not exhibit any interaction between the central Ni^{II} ion in the complex and the counter anion, and the chelate ring conformation was found to be $\delta\delta/\lambda\lambda$ (*racemic*), the same as those of complexes **1** and **2**. Thus, these findings may indicate a relationship between the accessibility of coordination of the fifth ligand and the chelate ring conformation in the Ni^{II} triad complexes.

The Ph_2Pqn complex **3** afforded orange platelet crystals when crystallized from acetonitrile/diethyl ether, but apparently more reddish crystals with a dichloromethane solvate molecule ($3 \cdot \text{CH}_2\text{Cl}_2$) when deposited by vapor diffusion of dichloromethane into an acetonitrile solution. We determined the crystal structures of both **3** and $3 \cdot \text{CH}_2\text{Cl}_2$ and found that the molecular structures of the complex cations are almost identical. A perspective drawing of the complex cation in **3** is shown in Figure 3 (and that of $3 \cdot \text{CH}_2\text{Cl}_2$ is in Figure S2). The MePhPqn complex $[\text{Ni}(\text{MePhPqn})_2](\text{BF}_4)_2$ (**4**) was obtained as red platelet crystals, and X-ray structural analysis (Figure 4) confirmed the product to be the *racemic* (*RR/SS*) diastereoisomer. The coordination plane around the Ni^{II} center is distorted toward a tetrahedral geometry in both **3** ($3 \cdot \text{CH}_2\text{Cl}_2$) and **4**. The dihedral angles between the planes defined by $\{\text{Ni}1, \text{P}1, \text{N}1\}$ and $\{\text{Ni}1, \text{P}2, \text{N}11\}$ are $19.7(3)^\circ$, $21.9(3)^\circ$, and $27.9(1)^\circ$ for complexes **3**, $3 \cdot \text{CH}_2\text{Cl}_2$, and **4**, respectively. This distortion results from the steric hindrance between the *ortho*-H atoms of mutually *cis*-positioned quinolyl groups (Figure 5), and has previously been observed in the crystal structures of $[\text{Pd}(\text{Me}_2\text{Pqn})_2](\text{BF}_4)_2$ ^[7] and $[\text{Pd}(\text{Ph}_2\text{Pqn})_2](\text{Cl}$ or $\text{Br})_2$.^[8] Such a tetrahedral distortion of the coordination plane (around 20°) forces the phenyl groups on the P atoms to become close enough for appreciable intramolecular stacking interactions (Figure 5, b). However, the crystal structure of the MePhPqn complex **4** is *racemic* (*RR/SS*) rather than *meso* (*RS*), the latter of which must be favorable for such an intramolecular stacking interaction. Furthermore, as the $\text{P}1\text{--Ni}1\text{--P}2$ angle of the Ph_2Pqn complex [**3**: $96.76(8)^\circ$; $3 \cdot \text{CH}_2\text{Cl}_2$: $96.54(8)^\circ$] is much larger than that of the MePhPqn complex [**4**: $93.26(4)^\circ$], there is probably no stacking interaction between these phenyl rings.

Table 1 lists selected bond lengths and angles for complexes **1–4**. The Ni–P and Ni–N bond lengths in the 2-aminoethylphosphane complexes **1** and **2** are similar to those in $[\text{Ni}(\text{Me}_2\text{Pea})_2][\text{NiCl}_4]$ [av. Ni–P: $2.148(4)$ Å; av. Ni–N: $1.977(12)$ Å]. We expected that the steric requirement of the phenyl substituent and/or the strong *trans* influence of the phosphanyl donor group might change these bond lengths, but only relatively small differences are observed for the Ni–P and Ni–N bond lengths between all $[\text{Ni}(\text{P–N})_2]^{2+}$ complexes. On the other hand, the $\text{P}1\text{--Ni}1\text{--P}2$ bond angles are indeed affected by the steric requirement of the phosphane substituents {cf. **1** $98.79(2)^\circ > \mathbf{2}$ $94.72(3)^\circ > [\text{Ni}(\text{Me}_2\text{Pea})_2][\text{NiCl}_4]$ $92.2(1)^\circ$ }. The Ni–P and Ni–N bond lengths in **1** are also similar to those in

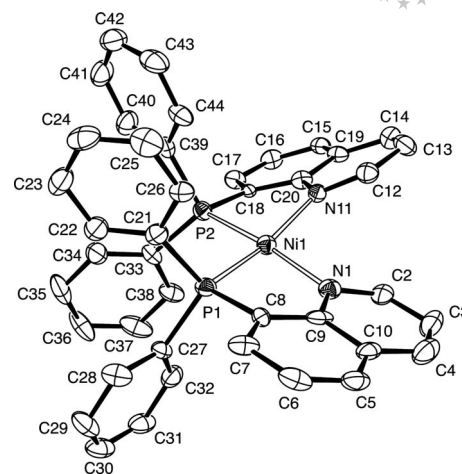


Figure 3. An ORTEP view (50% probability level, hydrogen atoms omitted) of the cationic moiety in $[\text{Ni}(\text{Ph}_2\text{Pqn})_2](\text{BF}_4)_2$ (**3**).

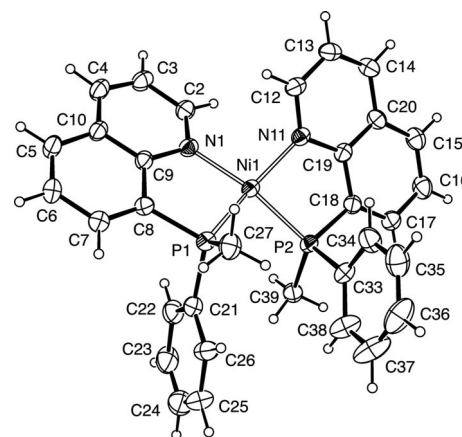


Figure 4. An ORTEP view (50% probability level) of the cationic moiety in $[\text{Ni}(\text{MePhPqn})_2](\text{BF}_4)_2$ (**4**).

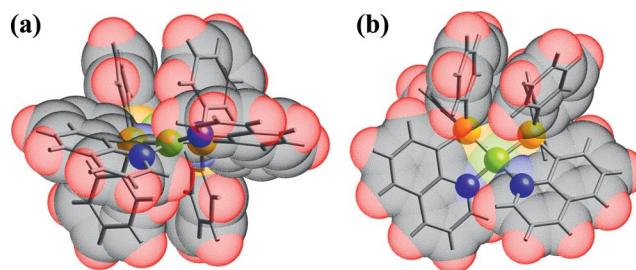


Figure 5. (a) Side and (b) top views of a space-filling model of the cationic moiety in $[\text{Ni}(\text{Ph}_2\text{Pqn})_2](\text{BF}_4)_2$ (**3**).

$[\text{Ni}(\text{Ph}_2\text{PCH}_2\text{py})_2][\text{NiCl}_4]$ [av. Ni–P: $2.160(3)$ Å; av. Ni–N: $1.956(6)$ Å].^[19] It should also be noted that the Ni–P and Ni–N bond lengths of the 2-aminoethylphosphane and 8-quinolylphosphane complexes (**1** and **2** vs. **3** and **4**) are rather similar, whereas the spectroscopic and electrochemical properties of these complexes exhibit remarkable differences, as discussed below.

Table 1. Selected bond lengths [Å] and angles [°] for complexes 1–4.

	1	2	3	3·CH ₂ Cl ₂	4
Ni1–P1	2.1584(5)	2.1526(7)	2.168(2)	2.180(2)	2.162(1)
Ni1–P2	2.1614(5)	2.1475(8)	2.177(2)	2.191(2)	2.151(1)
Ni1–N1	1.967(2)	1.969(2)	1.954(6)	1.969(4)	1.954(3)
Ni1–N11	1.959(2)	1.970(2)	1.949(5)	1.943(4)	1.977(3)
P1–Ni1–P2	98.79(2)	94.72(3)	96.76(8)	96.54(8)	93.26(4)
N1–Ni1–N11	89.41(6)	91.8(1)	95.0(2)	97.3(2)	99.0(1)
P1–Ni1–N1	85.73(5)	86.57(7)	86.6(2)	83.9(2)	87.4(1)
P2–Ni1–N11	86.06(5)	87.08(8)	84.6(2)	86.0(2)	86.6(1)
P2–Ni1–N1	175.46(5)	177.07(8)	168.0(2)	165.3(2)	162.2(1)
P1–Ni1–N11	175.08(5)	175.58(8)	165.3(2)	165.2(2)	159.3(1)

Spectroscopic Properties and Molecular Structures in Solution

As mentioned above, the ¹H NMR spectra for the 2-aminoethylphosphane complexes (**1** and **2**) in CD₃CN were typical of diamagnetic complexes. This fact suggested that the square-planar coordination geometry around the Ni^{II} center would be retained in solution. The MePhPea complex **2** afforded two diastereoisomers (*rac* and *meso*), which could be separated by fractional recrystallization. The *rac* isomer (*rac-2*), the structure of which was confirmed by single-crystal X-ray analysis, showed the P–CH₃ resonance at $\delta = 1.05$ ppm as a virtual triplet. This virtual coupling pattern of the P–CH₃ group is normal for square-planar Ni^{II} and Pd^{II} complexes with a *cis*(*P,P*) configuration.^[6] The other isomer (*meso-2*) gave the corresponding resonance at $\delta = 1.85$ ppm (virtual triplet, Figure S1). The relatively large difference in their chemical shifts could result from the ring current effect of the phenyl ring in the mutually *cis*-positioned MePhP donor groups, as seen in Figure 2. Both *rac-2* and *meso-2* showed rather broad resonances for the 2-aminoethyl moieties (NH₂CH₂CH₂P) at 23 °C, similar to the case of complex **1** (see above). At –16.5 °C, however, each resonance became separated into two broad resonances (Figure S1), thus indicating that there is a fast puckering motion of the five-membered chelate ring at ambient temperature. In addition, it should be noted that no isomerization was observed between *rac-2* and *meso-2* in CD₃CN; the relative intensities of the resonances for these two species were independent of temperature (from –16.5 to 40 °C) and unchanged on standing for several days at ambient temperature. Thus, the square-planar coordination of 2-aminoethylphosphanes toward Ni^{II} with a *cis*(*P,P*) configuration is robust in acetonitrile solution.

The 8-quinolyphosphane complexes (**3** and **4**) are diamagnetic in the solid state (up to 400 K measured). The ¹H NMR spectrum of the Ph₂Pqn complex **3** in CD₃NO₂ shows reasonably sharp resonances for the phenyl and quinoyl protons at $\delta = 7.33$ – 8.90 ppm (Figure S3), thus indicating a diamagnetic nature in solution. The distorted square-planar coordination geometry found in the crystal structure analysis of **3** therefore seems to be maintained in nitromethane solution. However, the ¹H NMR spectrum of **3** in CD₃CN shows very broad signals in the range $\delta = -20$ to 30 ppm (Figure S3). A similar paramagnetic behavior in

CD₃CN was also observed for the MePhPqn complex **4**. Temperature-dependent ¹H NMR spectra of complex **3** in CD₃CN (Figure S3) suggest that it exists as an equilibrium mixture of diamagnetic and paramagnetic species. The diamagnetic species must have a distorted square-planar coordination geometry as in CD₃NO₂, whereas two possibilities can be considered for the paramagnetic species. One is the existence of an acetonitrile adduct having a five-coordinate square-pyramidal geometry or a six-coordinate octahedral coordination geometry. We attempted to detect such complexes by ESI-TOF mass spectrometry but were unsuccessful. The other possibility for the observed paramagnetism is a much stronger tetrahedral distortion of the Ni^{II} coordination geometry. As both diamagnetic and paramagnetic species were detected at lower temperatures, there should be a moderately high-energy transition state, which might be caused by a collision of the phenyl groups arising from the tetrahedral distortion. This explanation seems to be plausible, but we are unsure as to why such a tetrahedral distortion occurs in acetonitrile but not in nitromethane.

The ¹H NMR spectrum of the MePhPqn complex **4** in CD₃NO₂ (Figure S4) was also indicative of diamagnetism of the solutes, and the temperature-dependent spectral change suggested that they were an equilibrium mixture of two species (*rac-4* and *meso-4*). Two P–CH₃ resonances from the respective species were observed at $\delta = 1.58$ and 2.48 ppm (at 21 °C); this difference in chemical shifts is similar to that of *rac-2* and *meso-2* (see above) and results from the ring current effect of the mutually *cis*-positioned MePhP donor groups. Thus, the species having a higher-field P–CH₃ resonance would be assigned as *rac-4* (Figure 4). The equilibrium fraction of *rac-4* (over *meso-4*) became larger at higher temperature (*rac-4*/*meso-4* = 1.7 at 0 °C and 5.5 at 40 °C; Figure S4), which suggests that the 8-quinolyphosphane complexes **3** and **4** are rather labile towards structural change in solution, in contrast to the robustness of 2-aminoethylphosphane complexes **1** and **2**.

The UV/Vis absorption spectra of complexes **1** and **2**^[20] in acetonitrile are shown in Figure 6. In accordance with the above ¹H NMR study, these spectra are similar in pattern to those in nitromethane and the diffuse-reflectance spectra of the solid samples (Figure S5). Square-planar Ni^{II} complexes often exhibit a single, broad unsymmetrical band in the region 20000–25000 cm^{–1}, which can be assigned to the superposition of the d–d transition bands; the band en-

ergy corresponds to Δ_{oct} (ligand-field strength) of the ligand to a first approximation.^[21a] The Ph₂Pea (**1**) and MePhPea (**2**) complexes exhibit such an absorption band at 24100 and 25300 cm⁻¹, respectively, with an intensity, ϵ , of around 400 M⁻¹ cm⁻¹ (Figure 6).

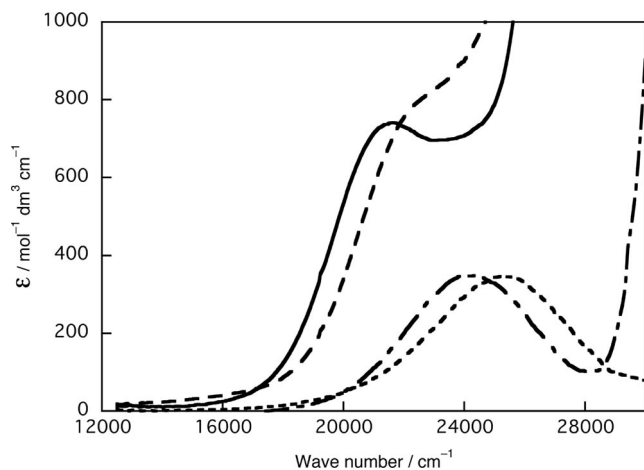


Figure 6. Absorption spectra of 2-aminoethylphosphane complexes **1** (---) and **2** (····) in acetonitrile and those of 8-quinolylphosphane complexes **3** (—) and **4** (-·-·-) in nitromethane at room temperature.

As seen above, complexes **3** and **4** show a remarkable solvent dependence in their structures in solution. In acetonitrile, complex **3** shows a broad absorption band at 19900 cm⁻¹, and complex **4** exhibits two broad shoulders at around 20500 and 25500 cm⁻¹ (Figure S6). These spectra are apparently different in pattern from the diffuse-reflectance spectra of the solid samples (Figure S6), although the spectra in nitromethane and the solid diffuse-reflectance spectra are similar in pattern for both complexes. These observations are consistent with the results of the ¹H NMR measurements above: the distorted square-planar coordination geometry of complexes **3** and **4** is maintained in nitromethane, whereas in acetonitrile they exist as an equilibrium mixture with a paramagnetic species (a five- or six-coordinate acetonitrile adduct or a tetrahedral complex). The Ph₂Pqn (**3**) and MePhPqn (**4**) complexes in nitromethane exhibit an absorption band at 21700 cm⁻¹ and a shoulder absorption at around 22000 cm⁻¹ ($\epsilon \approx 800$ M⁻¹ cm⁻¹), respectively (Figure 6). These band energies indicate weaker ligand-field strengths of 8-quinolylphosphanes than 2-aminoethylphosphane [Δ_{oct} (cm⁻¹) = 25300 (MePhPea) > 24100 (Ph₂Pea) >> ca. 22000 (MePhPqn) > 21700 (Ph₂Pqn)].

Electrochemical Properties

Figure 7 shows cyclic voltammograms of complex **3** in acetonitrile and nitromethane (those for the other complexes are shown in Figure S7). The redox potentials ($E_{1/2}$ vs. Fc^{+/0}) and the difference in potential between anodic and cathodic peaks (ΔE_p) are listed in Table 2. These data are indicative of the quasi-reversible one-electron reduction

process of the Ni^{II} complexes, except for MePhPea complex **2**,^[20] which gives an irreversible voltammogram at very low potential, presumably because of immediate decomposition of the reduced product. As seen in Figure 7 (and Table 2), the electrochemical behavior of complex **3** shows a small but clear solvent dependence ($\Delta E_{1/2} \approx 20$ mV and $\Delta \Delta E_p \approx 10$ mV). These differences are likely to be caused by the different molecular structures of the Ph₂Pqn complex in acetonitrile and nitromethane solutions, as described above.

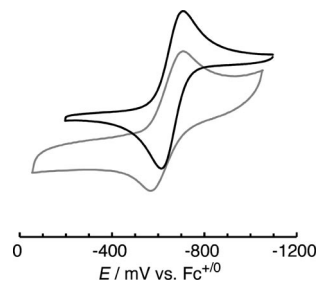


Figure 7. Cyclic voltammograms of [Ni(Ph₂Pqn)₂](BF₄)₂ (**3**) in acetonitrile (black) and nitromethane (gray) at 25 °C. [complex] = 1.0 × 10⁻³ M, I = 0.1 M (TBABF₄).

Table 2. Redox potential of Ni complexes (in 0.1 M TBABF₄ solution in acetonitrile or nitromethane at 298.2 ± 0.2 K).^[a]

Complex/solvent	Assignment	$E_{1/2}$ [mV]	ΔE_p [mV]
1 /CH ₃ CN	[Ni(Ph ₂ Pea) ₂] ^{2+/+}	-1147	87
2 /CH ₃ CN ^[b]	[Ni(MePhPea) ₂] ^{2+/+}	-1389	59 ^[b]
3 /CH ₃ CN	[Ni(Ph ₂ Pqn) ₂] ^{2+/+}	-660	98
3 /CH ₃ NO ₂	[Ni(Ph ₂ Pqn) ₂] ^{2+/+}	-640	109
4 /CH ₃ CN	[Ni(MePhPqn) ₂] ^{2+/+}	-898	98

[a] vs. Fc^{+/0}. [b] Irreversible process due to decomposition of the reduced species.

The reduction potentials of these Ni^{II} complexes are largely dependent on the type of phosphane ligands. Thus, substitution of methyl for phenyl on a P donor atom induces an approximately 240 mV negative shift in the redox potential, while 8-quinolylphosphane complexes exhibit less negative (by ca 490 mV) redox potentials than the corresponding 2-aminoethylphosphane complexes. This behavior is consistent with the order of the ligand-field strengths observed by absorption spectroscopy: MePhPea (**2**) > Ph₂Pea (**1**) > MePhPqn (**4**) > Ph₂Pqn (**3**).

Preparation and Crystal Structure of Nickel(I) Ph₂Pqn Complex

Reduction of Ph₂Pqn complex **3** with Zn powder^[22] in acetonitrile afforded a dark red solution, from which a dark red precipitate could be isolated on addition of deaerated water. As the cyclic voltammogram of this product (in acetonitrile) was almost identical to that of complex **3**, it was assumed to be the corresponding Ni^I complex of [Ni(Ph₂Pqn)₂]BF₄ (**5**). The UV/Vis spectrum of **5** in acetonitrile shows shoulder absorptions at around 11500 and 14500 cm⁻¹ with intensities of around 200 M⁻¹ cm⁻¹ (Figure S8). This spectral pattern is similar to the diffuse-reflectance

spectrum of a solid sample of complex **5**, thus indicating a similar molecular structure of the Ni^I complex cation in the solid state and in acetonitrile.

The crystal structure of complex **5** was determined by X-ray analysis. The asymmetric unit (triclinic space group $P\bar{1}$, $Z = 2$) contains an $[\text{Ni}(\text{Ph}_2\text{Pqn})_2]^+$ cation and a BF_4^- anion. The structure of the $[\text{Ni}(\text{Ph}_2\text{Pqn})_2]^+$ moiety is shown in Figure 8. The coordination geometry around the Ni^I center is distorted tetrahedral; the dihedral angle between the $\{\text{Ni}1, \text{P}1, \text{N}1\}$ plane and the $\{\text{Ni}1, \text{P}2, \text{N}11\}$ plane is $57.6(1)^\circ$, and that between the least-squares quinoyl rings is $61.06(9)^\circ$. The $\text{P}1\text{--Ni}1\text{--P}2$ bond angle is $115.67(4)^\circ$. If a regular tetrahedral geometry around the Ni center is assumed, a large steric hindrance between the phenyl substituents would be expected. Thus, to reduce such a steric interaction effectively, the coordination geometry is distorted by around 30° toward a *syn* structure.^[23] A Jahn–Teller effect of the d⁹ tetrahedral complex may be another reason for this distortion.^[21b]

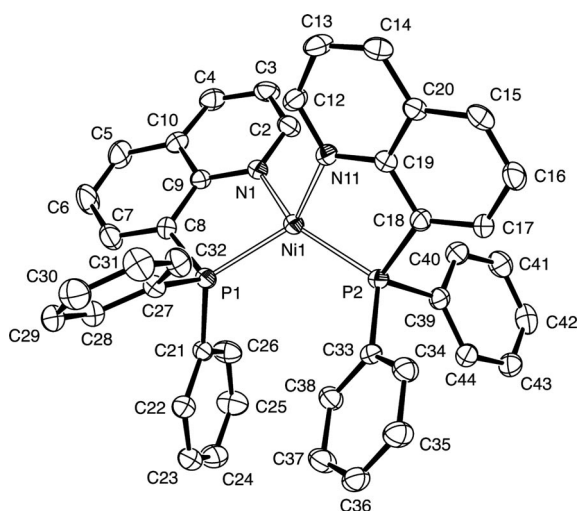


Figure 8. An ORTEP view (30% probability level, hydrogen atoms omitted) of the cation in $[\text{Ni}(\text{Ph}_2\text{Pqn})_2]\text{BF}_4$ (**5**). Selected bond lengths [Å] and angles [°]: Ni1–P1 2.230(1), Ni1–P2 2.224(1), Ni1–N1 2.003(3), Ni1–N11 2.017(3); P1–Ni1–P2 115.67(4), N1–Ni1–N11 96.48(12), P1–Ni1–N1 86.22(9), P2–Ni1–N11 86.19(9), P1–Ni1–N11, 134.72(9), P2–Ni1–N1 145.92(9).

The Ni–P and Ni–N bond lengths in complex **5** are 2.224(1)–2.230(1) and 2.003(3)–2.017(3) Å, respectively, around 0.05 Å longer than the corresponding bonds in the Ni^{II} complex **3**. This can be explained by the difference in ionic radii between Ni⁺ and Ni²⁺.^[24] The Ni–P bond lengths in $[\text{Ni}(\text{PMe}_3)_4]\text{BPh}_4$, where the coordination geometry of Ni^I is also distorted tetrahedral, are reported to be 2.211(3)–2.221(3) Å.^[25] The Ni–P bonds in the three-coordinate iminobenzylamide complex $[\text{Ni}^{\text{I}}(\text{ArN}=\text{CHC}_6\text{H}_4\text{N}-\text{Ar}')(\text{PPh}_3)]$ are 2.210(1) and 2.233(2) Å.^[26] Several other Ni^I complexes containing the bidentate phosphane ligand *t*Bu₂PCH₂CH₂P*t*Bu₂ (dtbpe) have been reported by Hilhouse et al., and the Ni^I–P bond lengths in the chlorido-bridged dimer $[(\text{dtbpe})\text{Ni}(\mu\text{-Cl})_2]$ are 2.210(1)–

2.216(1) Å.^[27] Compared with these examples, the present Ni^I–P bond lengths in complex **5** [av. 2.227(1) Å] seem to be normal for Ni^I phosphane complexes.

Conclusions

We have characterized four nickel(II) complexes of the type $[\text{Ni}(\text{P–N})_2](\text{BF}_4)_2$, where P–N is a 2-aminoethylphosphane or 8-quinolyphosphane ligand. The coordination geometry of the 2-aminoethylphosphane complexes **1** and **2** is square planar with a *cis*(*P,P*) configuration in the solid state and in acetonitrile solution. It seems that the coordination bonds of Ph₂Pea and MePhPea to a Ni^{II} ion are robust in solution. The diastereoisomers (*rac* and *meso*) of *cis*(*P,P*)- $[\text{Ni}(\text{MePhPea})_2](\text{BF}_4)_2$ (**2**) have been separated by fractional recrystallization and the crystal structure of *rac*-**2** determined by X-ray analysis.

In contrast, the 8-quinolyphosphanes result in distorted square-planar Ni^{II} complexes (**3** and **4**) because of the steric repulsion between the *ortho*-H atoms in the mutually *cis*-positioned quinoyl rings. This distortion makes the σ - and π -overlaps between Ni^{II} 3d and ligand orbitals ineffective, therefore the ligand-field strengths of the 8-quinolyphosphanes must be weaker in these complexes. In agreement with this conclusion, complexes **3** and **4** exhibit fluxional behavior in solution. The distorted square-planar geometry seems to be maintained in nitromethane as the absorption spectra in nitromethane are similar in pattern to the diffuse-reflectance spectra of the solid samples. Typical diamagnetic ¹H NMR spectra are also observed in CD₃NO₂, but the temperature-dependent ¹H NMR spectra of *cis*(*P,P*)- $[\text{Ni}(\text{MePhPqn})_2](\text{BF}_4)_2$ (**4**) indicate that this complex exists as an equilibrium mixture of *rac* and *meso* diastereoisomers. In acetonitrile, however, these complexes show paramagnetic behavior, presumably arising either from the coordination of solvent acetonitrile molecule(s) to form a five- or six-coordinate complex or the stronger tetrahedral distortion of the coordination geometry.

The weaker ligand-field strengths of 8-quinolyphosphanes than 2-aminoethylphosphanes are shown experimentally by the d–d transition energies observed by absorption spectroscopy: Ph₂Pqn < MePhPqn < Ph₂Pea < MePhPea. This order is consistent with that of the Ni^{III/I} redox potential of the complexes. The most readily reducible Ph₂Pqn complex (**3**) affords the corresponding nickel(I) complex $[\text{Ni}(\text{Ph}_2\text{Pqn})_2]\text{BF}_4$ (**5**). The molecular structure of this Ni^I complex, which contains two bidentate phosphane ligands, is distorted tetrahedral because of the steric repulsion caused by the phenyl substituents and/or a Jahn–Teller effect of the ideally tetrahedral d⁹ complex.

Experimental Section

Materials and Measurements: All solvents used during preparation of the phosphanes and their complexes were dried with appropriate drying agents and distilled prior to use. The P–N-type hybrid li-

gands Ph₂Pea (previously abbreviated as edpp), MePhPea,^[12c] Ph₂Pqn,^[28] and MePhPqn^[17] were synthesized according to literature methods.

¹H NMR spectra were acquired on a Varian Mercury 300 spectrometer. Chemical shifts were referenced to the residual ¹H NMR signals of the deuterated solvents and are reported with respect to TMS. The ³¹P{¹H} NMR spectra were obtained on the same spectrometer, using 85% H₃PO₄ as an external reference for the ³¹P NMR chemical shifts. Absorption spectra were recorded with a Jasco V-550 spectrophotometer at room temperature. Diffuse-reflectance spectra of the solid samples were obtained on the same spectrophotometer using an integration sphere (Jasco ISN-470). Cyclic voltammograms were measured at 25.0(2) °C on a BAS-100B/W electrochemical analyzer in acetonitrile or nitromethane solution ([complex] = 1.0 mM, 0.1 M TBABF₄). A platinum disk (ϕ 1.8 mm), a platinum wire, and a Ag/AgNO₃ electrode were used as the working, auxiliary, and reference electrodes, respectively. The redox potentials of the samples were calibrated with respect to the redox signal for the ferrocenium/ferrocene couple.

[Ni(Ph₂Pea)₂](BF₄)₂ (1): A methanol solution (50 mL) of Ni(BF₄)₂·6H₂O (1.51 g, 4.44 mmol) was added with stirring to a suspension of Ph₂Pea (2.16 g, 9.42 mmol) in methanol (50 mL). The mixture was refluxed for 30 min and then cooled to 0 °C. The resulting yellow precipitate was collected by filtration, washed with methanol and diethyl ether, and dried in vacuo; yield 1.58 g (51.5%). C₂₈H₃₂B₂F₈N₂NiP₂ (690.83): calcd. C 48.7, H 4.67, N 4.06; found C 48.4, H 4.53, N 4.33. ¹H NMR (300 MHz, CD₃CN, 21 °C): δ = 2.58 (br., 2 H, CH₂), 2.70 (br., 2 H, CH₂), 3.90 (br., 2 H, NH₂), 7.33–7.38 (m, 4 H, Ph), 7.48–7.53 (m, 6 H, Ph) ppm. ³¹P{¹H} NMR (152 MHz, CD₃CN, 21 °C): δ = 49.2 (br) ppm. UV/vis [solvent]: σ_{\max} ($\epsilon_{\max}/M^{-1}cm^{-1}$) = 24100 (349) [CH₃CN]; 24500 (575) cm⁻¹ [CH₃NO₂]. Crystals suitable for X-ray analysis were obtained from an acetonitrile solution by vapor diffusion of diethyl ether.

[Ni(MePhPea)₂](BF₄)₂ (2): Under an argon atmosphere, 1.01 g of (crude) MePhPea was added to an ethanol solution (100 mL) of Ni(BF₄)₂·6H₂O (1.03 g, 3.03 mmol), and the mixture stirred under reflux for 1 h. The resulting yellow solution was concentrated to about 10 mL under reduced pressure, and then cooled to 0 °C to afford the product as a yellow precipitate; yield 0.48 g (28%). C₂₀H₃₄B₂F₈N₂NiOP₂ (2·EtOH, 612.75): calcd. C 39.3, H 5.61, N 4.59; found C 39.1, H 5.29, N 4.25. ¹H NMR (300 MHz, CD₃CN, 23 °C): δ = 1.05 (virtual t, Me of *rac*-2), 1.85 (virtual t, Me of *meso*-2), 2.0–2.4 (br., CH₂ of *rac*-2 and *meso*-2), 2.6–3.2 (br., CH₂ of *rac*-2 and *meso*-2), 3.75 (br., NH₂ of *rac*-2 and *meso*-2), 7.13–7.35 (m, Ph of *meso*-2), 7.50–7.85 (m, Ph of *rac*-2) ppm. ³¹P{¹H} NMR (152 MHz, CD₃CN, 23 °C): δ = 38.3 (*rac*-2) and 39.1 (*meso*-2) ppm. UV/vis [solvent]: σ_{\max} ($\epsilon_{\max}/M^{-1}cm^{-1}$) = 25300 (347) cm⁻¹ [CH₃CN]. This product was found to be a mixture of diastereoisomers (*rac* and *meso*). To obtain suitable crystals for the X-ray diffraction analysis, the crude product was mixed with a minimum amount of dichloromethane and the insoluble precipitate quickly collected by filtration. The resulting yellow product was recrystallized from an acetonitrile solution by vapor diffusion of diethyl ether to give yellow columnar crystals of *rac*-2.

[Ni(Ph₂Pqn)₂](BF₄)₂ (3): A methanol solution (50 mL) of Ni(BF₄)₂·6H₂O (830 mg, 2.44 mmol) was added with stirring to a suspension of Ph₂Pqn (1.76 g, 5.62 mmol) in methanol (50 mL). The mixture was refluxed for 30 min and then cooled to 0 °C. The resulting reddish-brown precipitate was collected by filtration, washed with methanol, thf, and diethyl ether, and dried in vacuo; yield 1.17 g (56.2%). C₄₃H₃₆B₂F₈N₂NiOP₂ (3·MeOH, 891.01): calcd. C 57.7, H

4.07, N 3.14; found C 57.4, H 3.78, N 3.22. ¹H NMR (300 MHz, CD₃NO₂, 21 °C): δ = 7.36 (t, J = 7.5 Hz, 4 H, *m*-Ph), 7.57 (t, J = 7.5 Hz, 2 H, *p*-Ph), 7.78 (m, 4 H, *o*-Ph), 7.94 (m, 2 H, qn), 8.14 (m, 1 H, qn), 8.42 (d, J = 8.1 Hz, 1 H, qn), 8.72 (m, 1 H, qn), 8.88 (d, J = 7.5 Hz, 1 H, qn) ppm. ³¹P{¹H} NMR (152 MHz, CD₃NO₂, 21 °C): δ = 43.2 (br) ppm. UV/Vis [solvent]: σ_{\max} ($\epsilon_{\max}/M^{-1}cm^{-1}$) = 12400 (40), 19900 (160), and 26300^{sh} (ca. 900) [CH₃CN]; 21700 (741) cm⁻¹ [CH₃NO₂]. Crystals suitable for X-ray analysis were obtained from an acetonitrile solution by vapor diffusion of diethyl ether (orange platelet crystals of 3) or dichloromethane (red platelet crystals of 3·CH₂Cl₂).

[Ni(MePhPqn)₂](BF₄)₂ (4): A methanol solution (50 mL) of Ni(BF₄)₂·6H₂O (4.1 g, 0.012 mol) was added with stirring to an ethanol solution (100 mL) of (crude) MePhPqn (6.0 g). The mixture was refluxed for 1 h and then cooled to 0 °C. The resulting yellow precipitate was collected by filtration, washed with ethanol and diethyl ether, and dried in vacuo; yield 5.93 g (67%). C₃₂H₂₈B₂F₈N₂NiP₂ (734.83): calcd. C 52.3, H 3.84, N 3.81; found C 52.0, H 3.83, N 3.75. ¹H NMR (300 MHz, CD₃NO₂, 21 °C): δ = 1.58 (s, Me of *rac*-4), 2.48 (s, Me of *meso*-4), 7.19 (t, J = 7.5 Hz, qn of *meso*-4), 7.40–7.50 (m, qn of *meso*-4), 7.72 (t, J = 7.5 Hz, qn of *rac*-4), 7.80–8.10 (m, qn of *rac*-4 and *meso*-4), 8.44 (d, J = 8.1 Hz, qn of *rac*-4), 8.78 (m, qn of *rac*-4), 8.91 (d, J = 8.1 Hz, qn of *rac*-4) ppm. ³¹P{¹H} NMR (152 MHz, CD₃NO₂, 21 °C): δ = 32.2 (br) ppm. UV/Vis [solvent]: σ_{\max} ($\epsilon_{\max}/M^{-1}cm^{-1}$) = 12900 (10), 20500^{sh} (ca. 300), and 25500^{sh} (ca. 800) [CH₃CN]; 22000^{sh} (ca. 750) cm⁻¹ [CH₃NO₂]. Crystals suitable for X-ray analysis were obtained from an acetonitrile solution by vapor diffusion of diethyl ether.

[Ni(Ph₂Pqn)₂](BF₄)₂ (5): An acetonitrile solution (20 mL) of 3 (223 mg, 0.260 mmol) was stirred over Zn powder (ca. 1 g) at room temperature for 1 h under argon and then unreacted Zn powder was filtered off. The filtrate was concentrated under reduced pressure, and deaerated water (50 mL) was added to the concentrate. The resulting dark red precipitate was collected by filtration, washed with water and diethyl ether, and dried in vacuo; yield 152 mg (76%). UV/Vis [solvent]: σ_{\max} ($\epsilon_{\max}/mol^{-1}dm^3cm^{-1}$) = 11500^{sh} (ca. 200) and 14500^{sh} (ca. 270) cm⁻¹ [CH₃CN]. Crystals suitable for X-ray analysis were obtained by vapor diffusion of diethyl ether into a nitromethane solution.

Crystallography: X-ray diffraction data for complexes 1–5 were obtained at –73(2) °C on a Rigaku R-axis rapid imaging plate detector with graphite-monochromated Mo- K_{α} radiation (λ = 0.71073 Å). A suitable crystal was mounted with a cryoloop and flash-cooled in a cold nitrogen stream. Data were processed by the Process-Auto program package,^[29] and absorption corrections were applied by the empirical method.^[30] The structures were solved by either direct methods using SIR92^[31] or by a heavy-atom method using DIRDIF99-PATY,^[32] and refined on F^2 (with all independent reflections) using the SHELXL97 program.^[33] All non-H atoms were refined anisotropically, and H atoms were introduced at the positions calculated theoretically and treated with riding models. All calculations were carried out using the CrystalStructure software package.^[34] Crystal data are collected in Table 3.

CCDC-743141 (for 1), -743142 (for 2), -743143 (for 3), -743144 (for 3·CH₂Cl₂), -743145 (for 4), -743146 (for 5) contain the supplementary crystallographic data for this paper. These data can be obtained free of charge from The Cambridge Crystallographic Data Centre via www.ccdc.cam.ac.uk/data_request/cif.

Supporting Information (see also the footnote on the first page of this article): An ORTEP drawing of the cationic moiety in

Table 3. Crystal data for complexes.

Complex	1	2	3	3·CH ₂ Cl ₂	4	5
Chemical formula	C ₂₈ H ₃₂ B ₂ F ₈ ⁻ N ₂ NiP ₂	C ₁₈ H ₂₈ B ₂ F ₈ ⁻ N ₂ NiP ₂	C ₄₂ H ₃₂ B ₂ F ₈ ⁻ N ₂ NiP ₂	C ₄₃ H ₃₄ B ₂ Cl ₂ F ₈ ⁻ N ₂ NiP ₂	C ₃₂ H ₂₈ B ₂ F ₈ ⁻ N ₂ NiP ₂	C ₄₂ H ₃₂ BF ₄ ⁻ N ₂ NiP ₂
<i>M</i>	690.83	566.68	858.97	943.89	734.83	772.16
Crystal system	monoclinic	triclinic	monoclinic	orthorhombic	monoclinic	triclinic
<i>a</i> [Å]	9.3420(3)	8.5664(5)	14.121(7)	15.905(14)	9.1097(5)	8.837(2)
<i>b</i> [Å]	9.2833(4)	10.9473(6)	15.758(10)	17.949(11)	20.535(1)	11.967(3)
<i>c</i> [Å]	35.5768(14)	13.8767(8)	17.976(7)	28.80(2)	17.912(1)	17.554(4)
<i>α</i> [°]	90	79.256(2)	90	90	90	90.901(5)
<i>β</i> [°]	94.725(1)	79.886(2)	94.94(4)	90	104.597(1)	99.519(5)
<i>γ</i> [°]	90	79.508(2)	90	90	90	101.362(5)
<i>V</i> [Å ³]	3074.9(2)	1243.56(12)	3985(4)	8221(11)	3242.6(3)	1792.8(7)
<i>T</i> [K]	200(2)	200(2)	200(2)	200(2)	200(2)	200(2)
Space group	<i>P</i> 2 ₁ / <i>n</i>	<i>P</i> $\bar{1}$	<i>P</i> 2 ₁ / <i>c</i>	<i>Pbca</i>	<i>P</i> 2 ₁ / <i>n</i>	<i>P</i> $\bar{1}$
<i>Z</i>	4	2	4	8	4	2
<i>D</i> _{calc} [Mg m ⁻³]	1.492	1.497	1.432	1.525	1.505	1.430
<i>μ</i> (Mo- <i>K</i> _α) [mm ⁻¹]	0.806	0.977	0.638	0.752	0.770	0.686
<i>R</i> _{int}	0.0151	0.0151	0.1127	0.2015	0.0741	0.0719
Number of param./reflections	416/6767	301/5629	515/8795	542/9102	427/7348	470/8039
<i>R</i> 1 (<i>F</i> ²) [<i>F</i> _o ² > 2σ(<i>F</i> _o ²)] ^[a]	0.0325	0.0469	0.0886	0.0816	0.0686	0.0605
<i>wR</i> 2 (<i>F</i> ²) (all data) ^[b]	0.0822	0.1418	0.2218	0.0908	0.1869	0.1751

[a] $R1 = \sum ||F_o| - |F_c|| / \sum |F_o|$. [b] $wR2 = [\sum w(F_o^2 - F_c^2)^2 / \sum wF_o^2]^{1/2}$.

[Ni(Ph₂Pqn)₂](BF₄)₂·CH₂Cl₂ (3·CH₂Cl₂), ¹H NMR spectra, UV/Vis absorption spectra, and cyclic voltammograms of complexes 1–4.

Acknowledgments

We thank Mr. Keita Ariyoshi and Ms. Yuki Yamane (Okayama University) for ³¹P NMR and magnetic measurements, respectively. This work was supported by the Ministry of Education, Culture, Sports, Science, and Technology, Japan, (Grant-in-Aid for Scientific Research; grant numbers 16550055 and 20550064).

- [1] a) C. S. Slone, D. A. Weinberger, C. A. Mirkin, *Prog. Inorg. Chem.* **1999**, *48*, 233–350; b) P. Espinet, K. Soulantica, *Coord. Chem. Rev.* **1999**, *193–195*, 499–556; c) B. Goldfuss, *J. Organomet. Chem.* **2006**, *691*, 4508–4513.
- [2] S. E. Angell, C. W. Rogers, Y. Zhang, M. O. Wolf, W. E. Jones Jr., *Coord. Chem. Rev.* **2006**, *250*, 1829–1841.
- [3] a) J. Andrieu, J.-M. Camus, P. Richard, R. Poli, L. Gonsalvi, F. Vizza, M. Peruzzini, *Eur. J. Inorg. Chem.* **2006**, 51–61; b) C. Müller, R. J. Lachicotte, W. D. Jones, *Organometallics* **2002**, *21*, 1975–1981.
- [4] a) P. Papanthasiou, G. Salem, P. Waring, A. C. Willis, *J. Chem. Soc., Dalton Trans.* **1997**, 3435–3443; b) A. Habtemariam, B. Watchman, B. S. Potter, R. Palmer, S. Parsons, A. Parkin, P. Sadler, *J. Chem. Soc., Dalton Trans.* **2001**, 1306–1318.
- [5] a) D. B. Grotjahn, Y. Gong, L. Zakharov, J. A. Golen, A. L. Rheingold, *J. Am. Chem. Soc.* **2006**, *128*, 438–453; b) S. Dilsky, W. A. Schenk, *Eur. J. Inorg. Chem.* **2004**, 4859–4870; c) S. Jung, C. D. Brandt, H. Werner, *New J. Chem.* **2001**, *25*, 1101–1103.
- [6] T. Suzuki, A. Morikawa, K. Kashiwabara, *Bull. Chem. Soc. Jpn.* **1996**, *69*, 2539–2548.
- [7] T. Suzuki, K. Kashiwabara, J. Fujita, *Bull. Chem. Soc. Jpn.* **1995**, *68*, 1619–1626.
- [8] T. Suzuki, *Bull. Chem. Soc. Jpn.* **2004**, *77*, 1869–1876.
- [9] a) T. Suzuki, T. Kuchiyama, S. Kishi, S. Kaizaki, H. D. Takagi, M. Kato, *Inorg. Chem.* **2003**, *42*, 785–795; b) T. Suzuki, T. Kuchiyama, S. Kishi, S. Kaizaki, M. Kato, *Bull. Chem. Soc. Jpn.* **2002**, *75*, 2433–2439.
- [10] a) T. Suzuki, K. Fujiwara, H. D. Takagi, K. Kashiwabara, *Dalton Trans.* **2007**, 308–319; b) K. Kashiwabara, A. Morikawa, T. Suzuki, K. Isobe, K. Tatsumi, *J. Chem. Soc., Dalton Trans.* **1997**, 1075–1081; c) T. Suzuki, M. Rude, K. P. Simonsen, M. Morooka, H. Tanaka, S. Ohba, F. Galsøl, J. Fujita, *Bull. Chem. Soc. Jpn.* **1994**, *67*, 1013–1023.
- [11] a) T. Suzuki, J. Fujita, *Chem. Lett.* **1992**, 1067–1068; b) T. Suzuki, M. Kita, K. Kashiwabara, J. Fujita, *Bull. Chem. Soc. Jpn.* **1990**, *63*, 3434–3442.
- [12] a) I. Kinoshita, Y. Yokota, K. Matsumoto, S. Ooi, K. Kashiwabara, J. Fujita, *Bull. Chem. Soc. Jpn.* **1983**, *56*, 1067–1073; b) I. Kinoshita, K. Kashiwabara, J. Fujita, K. Matsumoto, S. Ooi, *Bull. Chem. Soc. Jpn.* **1981**, *54*, 2683–2690; c) K. Kashiwabara, I. Kinoshita, T. Ito, J. Fujita, *Bull. Chem. Soc. Jpn.* **1981**, *54*, 725–732; d) I. Kinoshita, K. Kashiwabara, J. Fujita, *Bull. Chem. Soc. Jpn.* **1980**, *53*, 3715–3716.
- [13] F. Galsøl, M. Kojima, T. Ishii, S. Ohba, Y. Saito, J. Fujita, *Bull. Chem. Soc. Jpn.* **1986**, *59*, 1701–1707.
- [14] a) R. Morris, A. Habtemariam, Z. Guo, S. Parsons, P. J. Sadler, *Inorg. Chim. Acta* **2002**, *339*, 551–559; b) M. Ito, M. Hirakawa, A. Osaku, T. Ikariya, *Organometallics* **2003**, *22*, 4190–4192; c) R. Ares, M. Lopez-Torres, A. Fernandez, D. Vazquez-Garcia, J. M. Vila, L. Naya, J. J. Fernandez, *J. Organomet. Chem.* **2007**, *692*, 4197–4208; d) N. Blaquiére, S. Diallo-Garcia, S. I. Gorelsky, D. A. Black, K. Fagnou, *J. Am. Chem. Soc.* **2008**, *130*, 14034–14035.
- [15] a) K. Issleib, D. Haferburg, *Z. Naturforsch., Teil B* **1965**, *20*, 916–918; b) K. Issleib, H. Oehme, *Chem. Ber.* **1967**, *100*, 2685–2693; c) K. Issleib, A. Kipke, V. Hahnfeld, *Z. Anorg. Allg. Chem.* **1978**, *444*, 5–20; d) K. Issleib, A. Kipke, *Z. Anorg. Allg. Chem.* **1980**, *464*, 176–186.
- [16] J. W. L. Martin, J. A. L. Palmer, S. B. Wild, *Inorg. Chem.* **1984**, *23*, 2664–2668.
- [17] a) G. Salem, S. B. Wild, *Inorg. Chem.* **1992**, *31*, 581–586; b) D. G. Allen, G. M. McLaughlin, G. B. Robertson, W. L. Steffen, G. Salem, S. B. Wild, *Inorg. Chem.* **1982**, *21*, 1007–1014.
- [18] a) W.-H. Sun, Z. Li, H. Hu, B. Wa, H. Yang, N. Zhu, X. Leng, H. Wang, *New J. Chem.* **2002**, *26*, 1474–1478; b) P. Wehman, H. M. A. van Donge, A. Hagos, P. C. J. Kamer, P. W. N. W. van Leeuwen, *J. Organomet. Chem.* **1997**, *535*, 183–193; c) A. A. Hudali, J. V. Kingston, H. A. Tayim, *Inorg. Chem.* **1979**, *18*, 1391–1394; d) T. Tsukuda, C. Nishigata, K. Arai, T. Tsubomura, *Polyhedron* **2009**, *28*, 7–12.
- [19] a) J. T. Migue, S. W. Hawbaker, *J. Chem. Crystallogr.* **1997**, *27*, 603–608; b) U. E. Z. Schäfer, *Z. Anorg. Allg. Chem.* **1968**, *359*, 67–77.

- [20] We used a crude mixture of *rac*-**2** and *meso*-**2** (ca. 2:1) for the spectrophotometric and electrochemical measurements in order to facilitate comparison of the properties with those of an equilibrium mixture of *rac*-**4** and *meso*-**4** in nitromethane (and presumably in acetonitrile, too). It can also be assumed that the spectroscopic and electrochemical properties of these *rac* and *meso* diastereoisomers are not significantly different.
- [21] a) B. N. Figgis, M. A. Hitchman, in: *Ligand Field Theory and Its Applications*, Wiley-VCH, New York, USA, **2000**, p. 211–214; b) B. N. Figgis, M. A. Hitchman, in: *Ligand Field Theory and Its Applications*, Wiley-VCH, New York, USA, **2000**, p. 158–160.
- [22] D. G. Holah, A. N. Hughes, B. C. Hui, C.-T. Kan, *Can. J. Chem.* **1978**, *56*, 2552–2559.
- [23] a) W. Klyne, V. Prelog, *Experientia* **1960**, *16*, 521–523; b) D. Casarini, C. Coluccini, L. Lunazzi, A. Mazzanti, *J. Org. Chem.* **2005**, *70*, 5098–5102.
- [24] There are no data available for the ionic or crystal radius of Ni^I, but a speculation from the crystal radii of Ni^{II}, Ni^{III}, and Ni^{IV} suggests a larger radius for Ni^I than for Ni^{II} (see: R. D. Shannon, *Acta Crystallogr., Sect. A* **1976**, *32*, 751–767).
- [25] A. Gleizes, M. Dartiguenave, Y. Dartiguenave, J. Galy, H. F. Klein, *J. Am. Chem. Soc.* **1977**, *99*, 1587–1589.
- [26] H.-Y. Wang, X. Meng, G.-X. Jin, *Dalton Trans.* **2006**, 2579–2585.
- [27] a) K. D. Kitiachvili, D. J. Mindiola, G. L. Hillhouse, *J. Am. Chem. Soc.* **2004**, *126*, 10554–10555; b) D. J. Mindiola, R. W. Terman, D. M. Jenkins, G. L. Hillhouse, *Inorg. Chim. Acta* **2003**, *345*, 299–308; c) D. J. Mindiola, G. L. Hillhouse, *J. Am. Chem. Soc.* **2001**, *123*, 4623–4624.
- [28] R. D. Feltham, H. G. Metzger, *J. Organomet. Chem.* **1971**, *33*, 347–355.
- [29] Rigaku Co. Ltd., *Process-Auto, Automatic Data Acquisition and Processing Package for Imaging Plate Diffractometer*, Akishima, Tokyo, Japan, **1998**.
- [30] T. Higashi, *ABSCOR, Empirical Absorption Correction based on Fourier Series Approximation*, Rigaku Corporation, Tokyo, Japan, **1995**.
- [31] A. Altomare, G. Cascarano, C. Giacovazzo, A. Guagliardi, M. C. Burla, G. Polidori, M. Camali, *J. Appl. Crystallogr.* **1994**, *27*, 435.
- [32] P. T. Beurskens, G. Admiraal, G. Beruskena, W. P. Bosman, S. Garcia-Granda, R. O. Gould, J. M. M. Smits, C. Smykalla, *PATY, The DIRDIF program system. Technical Report of the Crystallography Laboratory*, University of Nijmegen, The Netherlands, **1992**.
- [33] G. M. Sheldrick, *Acta Crystallogr., Sect. A* **2008**, *64*, 112–122.
- [34] Rigaku and Rigaku/MS, *CrystalStructure ver. 3.6.0. Crystal Structure Analysis Package*, Akishima, Tokyo, Japan and The Woodlands, TX, USA, **2000–2004**.

Received: August 5, 2009

Published Online: November 26, 2009